Electronic Supplementary Information:

Hollow MoS$_2$/Co nanopillars with boosted Li-ion diffusion rate and long-term cycling stability

Xunlu Wang [ab], Ruguang Ma *[ac] Minmin Wang,[d] Jin Wang,[d] Tongming Sun,[d] Lanping Hu,[d] Jinli Zhu,[d] Yanfeng Tan,[d] and Jiacheng Wang *[ab]

[a.] State Key Laboratory of High-Performance Ceramics and Superfine Microstructure, Shanghai Institute of Ceramics, Chinese Academy of Sciences, 1295 Dingxi Road, Shanghai 200050, China.

E-mail: jiacheng.wang@mail.sic.ac.cn; maruguang@mail.sic.ac.cn.

[b.] Center of Materials Science and Optoelectronics Engineering, University of Chinese Academy of Sciences, 100049 Beijing, China

Email: jiacheng.wang@mail.sic.ac.cn;

[c.] School of Materials Science and Engineering, Suzhou University of Science and Technology, 99 Xuefu Road Suzhou, 215011, China

Email: ruguangma@usts.edu.cn

[d.] College of Chemistry and Chemical Engineering, Nantong University, Nantong 226019, China

1. Experimental section

1.1. Preparation of hollow MoS_2/Co-0.1 nanopillars

All chemicals were analytical reagents and used directly without purification. First, we synthesized the $CoMoO_4$ nanorods as precursor via hydrothermal method at 140℃ for 6 h in 30 mL of deionized water containing 3 mmol nickel (II) nitrate hexahydrate and 3 mmol ammonium molybdate tetrahydrate as shown in Fig. S1. Then, when the as-synthesized $CoMoO_4$ nanorods were sulfureted with sulfur powder in a H_2/Ar (v/v, 5/95) atmosphere at 550 ℃ for 2 h, the inner Mo atoms diffused outward and formed MoS_2. As a result, MoS_2 nanosheets were grown directly on Co nanorods as shown in Fig. S2, which was named as MoS_2/Co-1 (the atomic ratio of Co and Mo is 0.92, Fig. S4). Finally, the hollow structured MoS_2/Co-0.1 was obtained by etching with suitable sulfuric acid (H_2SO_4). The hollow structured MoS_2/Co-0.01 was synthesized by etching with excessive sulfuric acid (H_2SO_4).

1.2. Characterization

The structure and morphology of the obtained samples were characterized by powder XRD (D8 ADVANCE, Cu Kα radiation), SEM (FEI Magellan 400), TEM, and HRTEM (JEM-2100F). The chemical composition of the products was analyzed by XPS measurements (ESCALAB) using Al Kα (hv = 1486.6 eV) radiation. Raman spectra were recorded by a DXR Raman Microscope (Thermal Scientific Co., USA) with 532 nm excitation length.

1.3. Electrochemical measurements

Electrochemical performances of the MoS_2/Co-based electrodes were tested by 2016-type coin cells packaged in an argon-filled glovebox. A mixed slurry (active materials: acetylene black: PVDF binder = 8:1:1 in weight) was coated onto clean copper foil and dried in a vacuum oven for 12 h to obtain the working electrode. The typical mass loading of the active materials was about 1.0 ± 0.2 mg cm^{-2}. The working electrodes were assembled into a half-cell using Li metal as counter electrode. The electrolyte was 1 M LiPF6 dissolved in the mixed solution containing ethyl carbonate (EC) and diethyl

carbonate (DEC) (1:1; v/v) and the separator was Whatman Glass Microfiber Filters. Galvanostatic discharge/charge curves were tested in the NEWARE battery testing system within the voltage range of 0.1-3.0 V (vs. Li/Li$^+$). EIS tests and CVs were conducted with an electrochemical workstation (CHI 760E). Finally, GITT tests were carried out in the NEWARE battery testing system with current density of 0.3 A g^{-1}, which was periodically interrupted every 5 min, with a 30 min rest period.
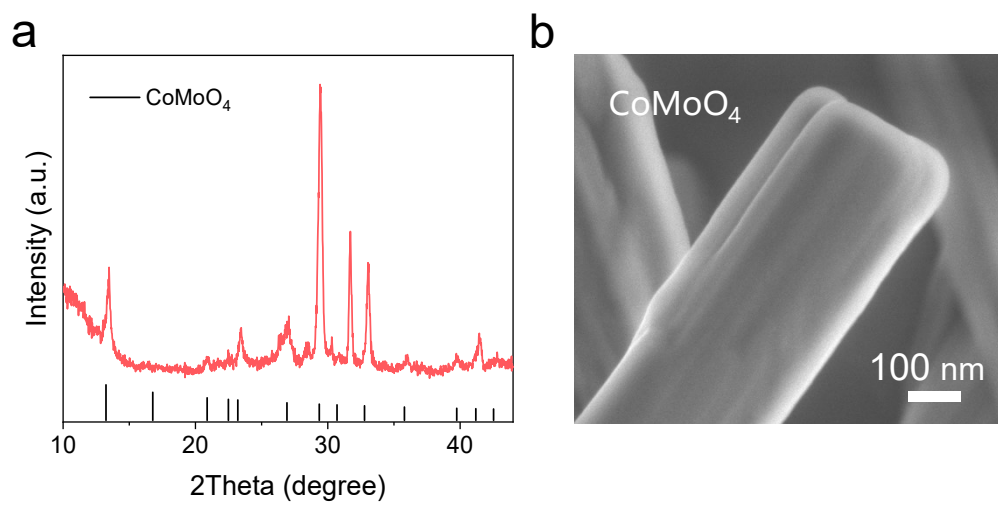
Fig. S1 a) XRD pattern, and b) SEM image of CoMoO$_4$.
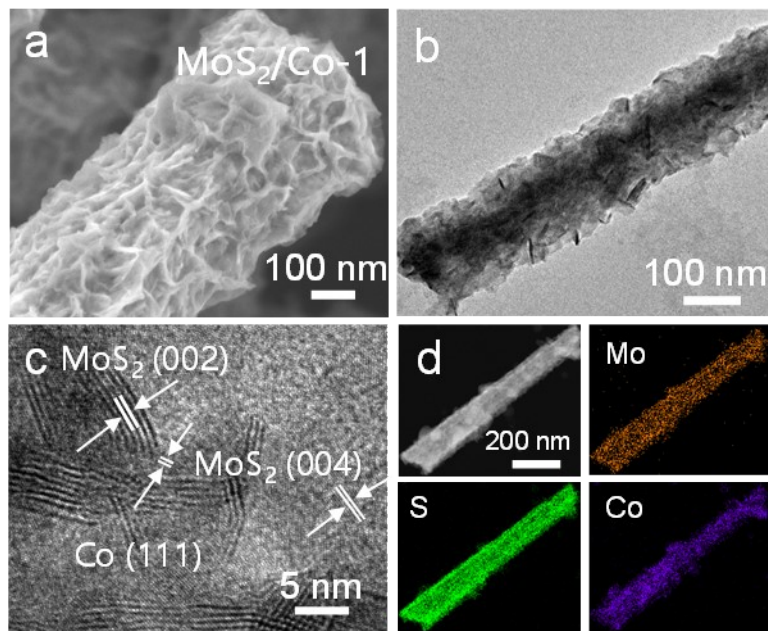
Fig. S2 a) SEM image, b) TEM image, c) HRTEM image, d) HAADF-STEM image

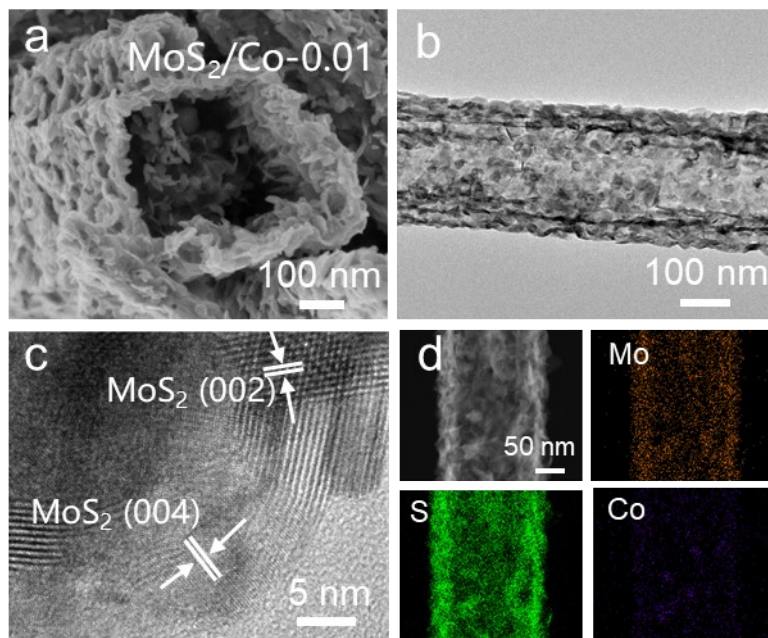and corresponding elemental mapping images of MoS$_2$/Co-1.

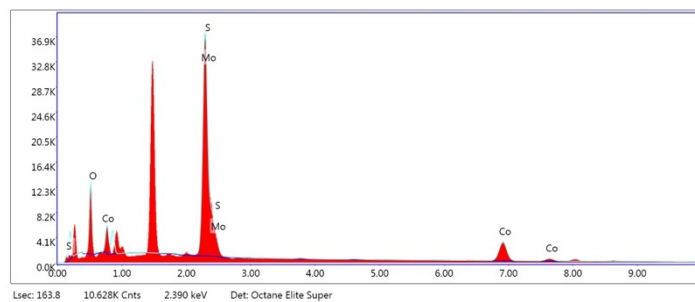**Fig. S3** a) SEM image, b) TEM image, c) HRTEM image, d) HAADF-STEM image and corresponding elemental mapping images of MoS$_2$/Co-0.01.
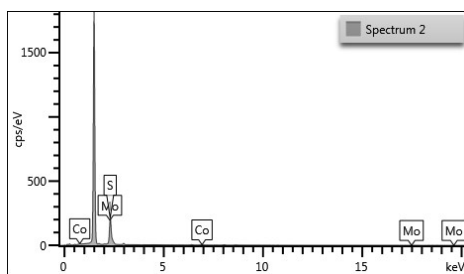
Fig. S4 EDX analysis of the MoS$_2$/Co-1.
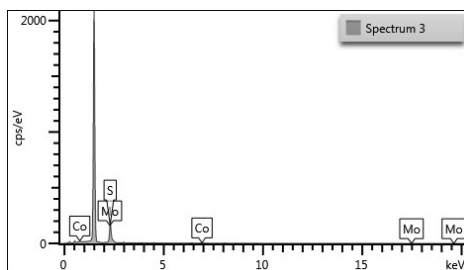

Fig. S5 EDX analyses of the MoS$_2$/Co-0.1.

Fig. S6 EDX analyses of the MoS$_2$/Co-0.01.
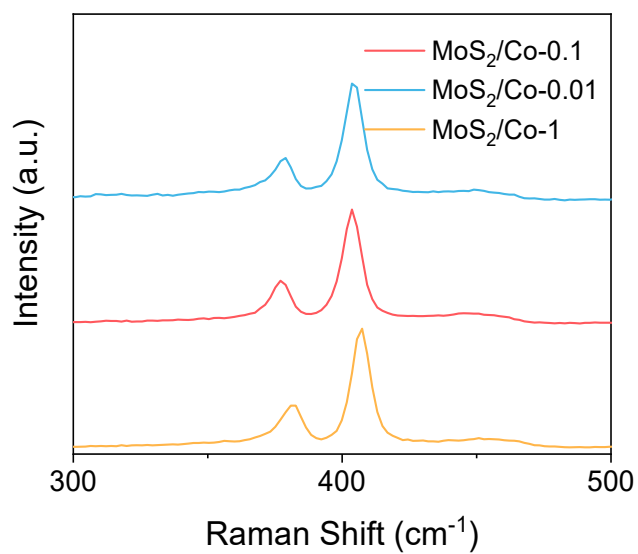
Fig. S7 Raman spectra of MoS_2/Co-0.1, MoS_2/Co-0.01 and MoS_2/Co-1.
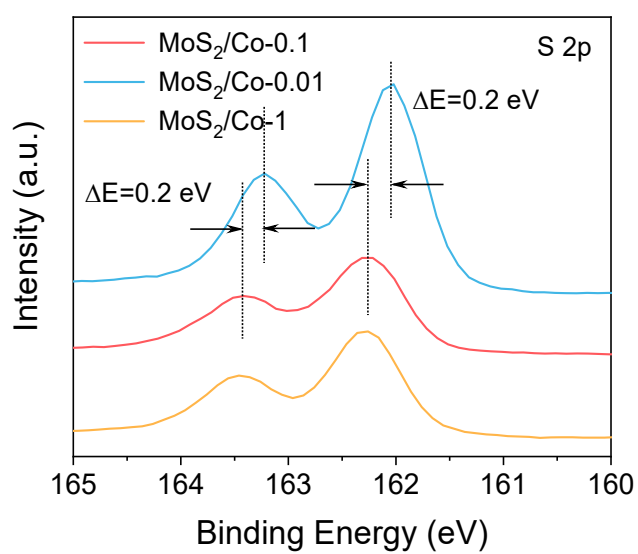

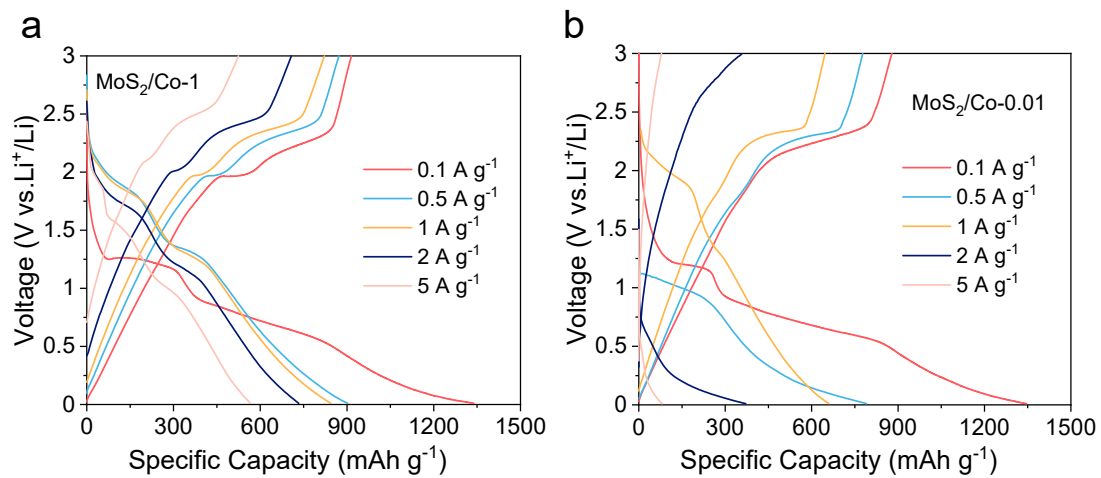**Fig. S8** S 2p XPS spectra of MoS_2/Co-0.1, MoS_2/Co-0.01 and MoS_2/Co-1.

Fig. S9 Charge/discharge curves of a) MoS₂/Co-1 and b) MoS₂/Co-0.01 at different
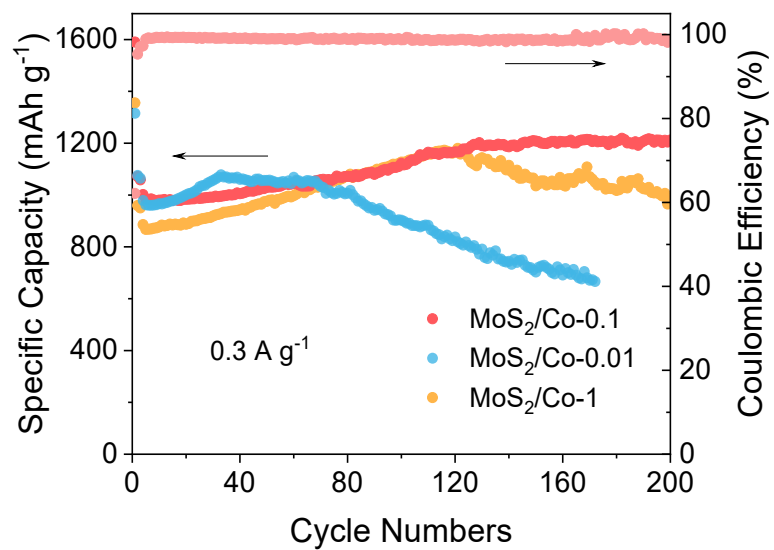
current densities.

Fig. S10 Cycling performance at a current density of 0.3 A g^{-1} for the MoS$_2$/Co-0.1, MoS$_2$/Co-0.01 and MoS$_2$/Co-1 electrodes.

Fig. S11 a) CV curves measured at different scan rates from 0.2 to 1 mV s^{-1}, b) *b* value according to the relationship of log(i) and log(v) at different peaks for MoS$_2$/Co-0.1.
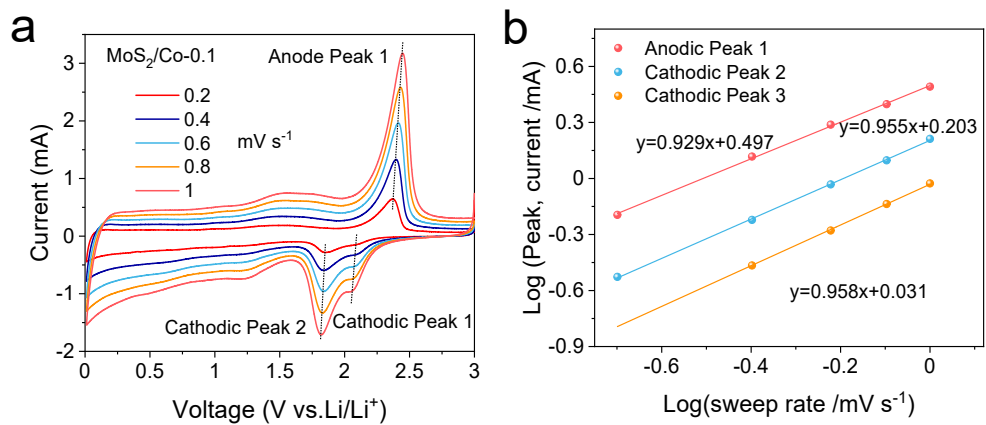
Fig. S12 a) CV curves measured at different scan rates from 0.2 to 1 mV s^{-1}, b) *b* value according to the relationship of log(i) and log(v) at different peaks, c) pseudocapacitive contribution (shaded area) at the scan rate of 0.6 mV s^{-1} and d) the ratio of pseudocapacitive contribution at different scan rates for MoS$_2$/Co-1.
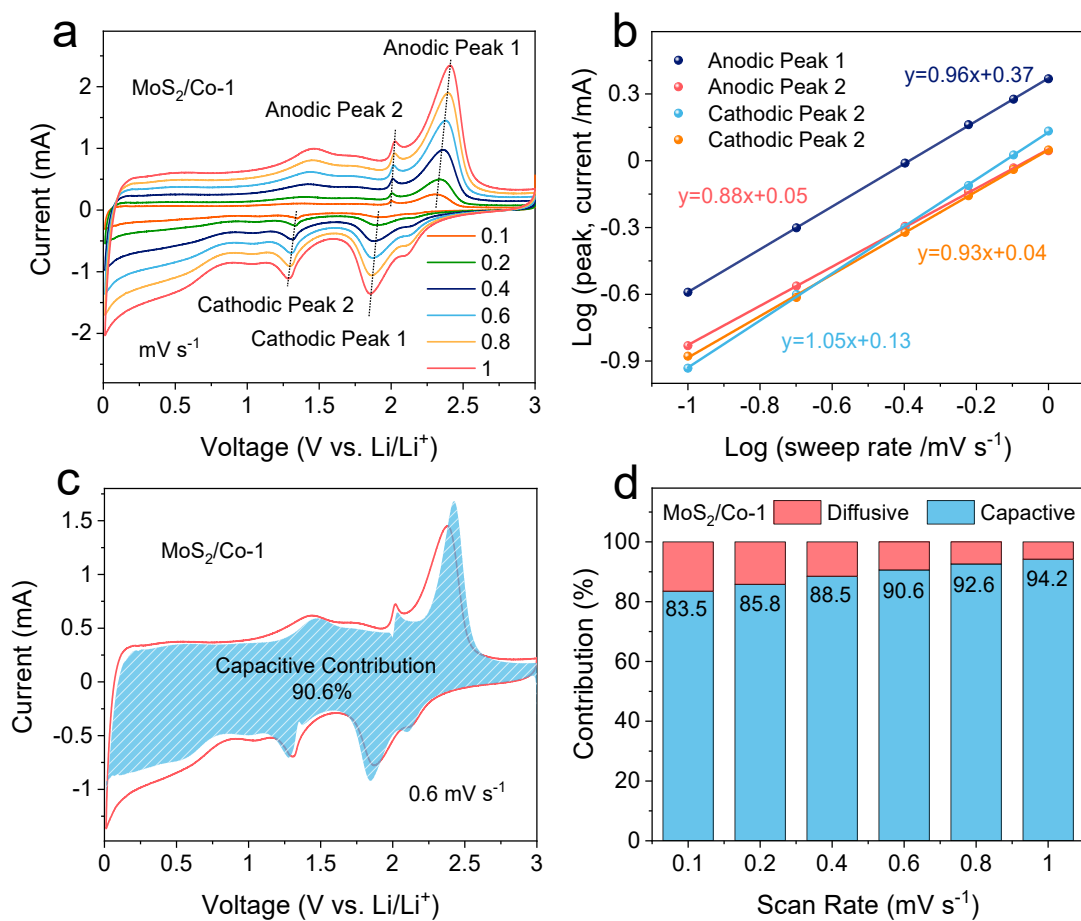
Fig. S13. a) CV curves measured at different scan rates from 0.2 to 1 mV s^{-1}, b) *b* value according to the relationship of log(i) and log(v) at different peaks, c) pseudocapacitive contribution (shaded area) at the scan rate of 0.6 mV s^{-1} and d) the ratio of pseudocapacitive contribution at different scan rates for MoS$_2$/Co-0.01.
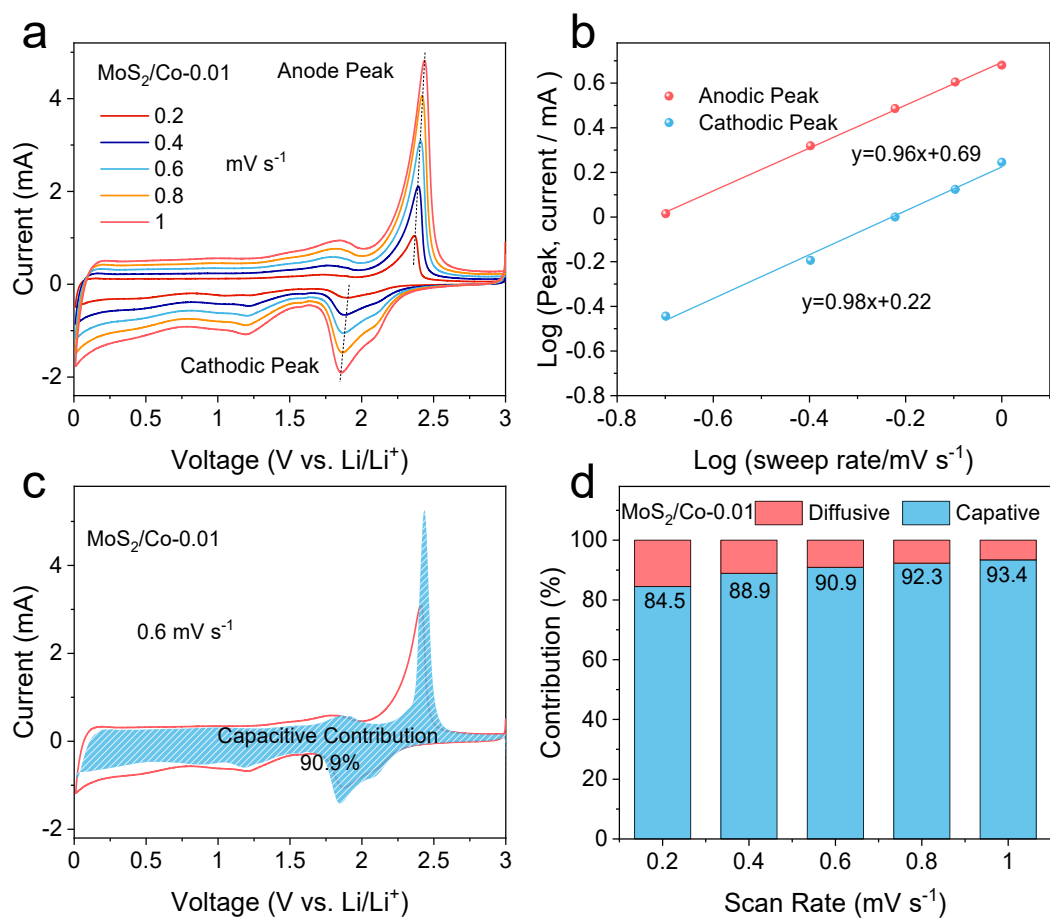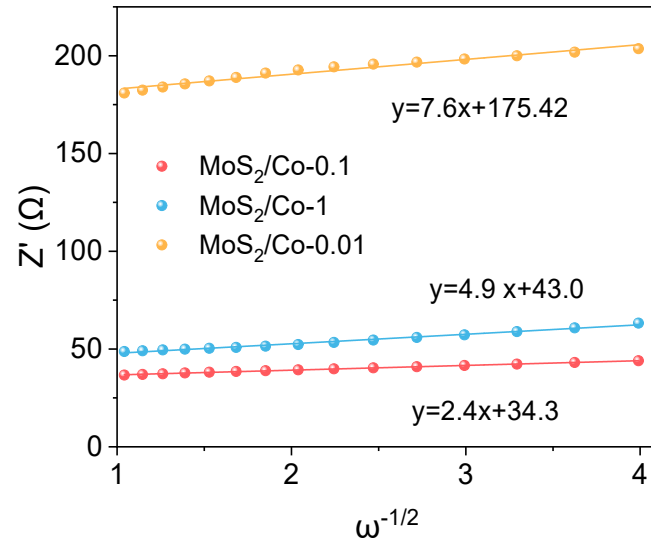
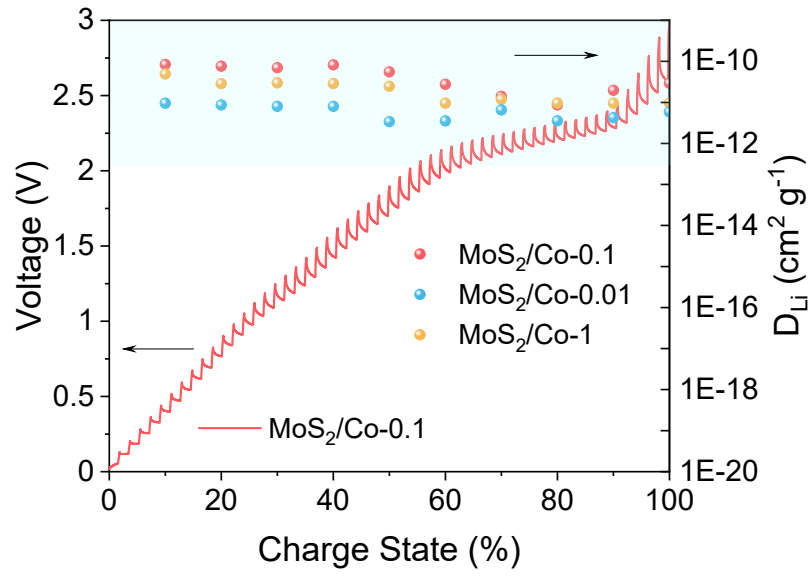**Fig. S14** Relationship between the real part of the impedance and $\omega^{-1/2}$ MoS$_2$/Co-0.1, MoS$_2$/Co-1 and MoS$_2$/Co-0.01.

Fig. S15 Charge profiles of MoS$_2$/Co-0.1, MoS$_2$/Co-1 and MoS$_2$/Co-0.01 electrodes in GITT test and the Li$^+$ diffusivity coefficient.

Table S1. The atomic ratio of Co and Mo in MoS_2/Co-0.1, MoS_2/Co-1 and MoS_2/Co-0.01.

Sample	Co/Mo
MoS_2/Co-1	0.92
MoS_2/Co-0.1	0.1
MoS_2/Co-0.01	0.01

Table S2. The R_{ct} values at different temperatures of MoS_2/Co-0.1 and MoS_2/Co-0.1, respectively.

Sample	R_{ct} 10 °C (Ω)	R_{ct} 20 °C (Ω)	R_{ct} 30 °C (Ω)	R_{ct} 40 °C (Ω)
MoS_2/Co-0.1	12.8	7.5	4.8	3.5
MoS_2/Co-0.01	181	101.8	68	35.9

Table S3. Tables of specific atomic content in MoS_2/Co-x

	Co	Mo	S
MoS_2/Co-1	21.11	23.16	55.73
MoS_2/Co-0.1	3.19	32.02	64.79
MoS_2/Co-0.01	0.38	33.7	65.92

Table S4. Statistics of MoS_2-based anode materials electrochemical measurements.

Sample	Current density (mA g-1)	Cycle number	Capacity retention (mAh g^{-1})	Ref.
MoS_2 nanosheet	400	500	1023	[3]
V4C3-MXene/MoS2/C	1000	450	662	[4]
1T-MoS2/C	1000	300	870	[5]
MoS2 -on-MXene	1000	100	580	[6]
MoS2 HollowNanospheres	500	100	1100	[7]
MoS2@N-CF nanosheets	1000	110	844	[8]
MoS2/NC-PNR	2000	700	520	[9]